III. SOLID STATE PHYSICS

Prof. W. P. Allis
Prof. S. C. Brown
Prof. C. W. Garland
Prof. G. G. Harvey
Dr. K. W. Billman
Dr. E. R. Pike
T. Higier
L. L. Isaacs
J. Silverman
R. Weber

A. SOFT X-RAY SPECTROSCOPY

Construction has been proceeding on a new ultra-high-vacuum soft X-ray spectrograph for the study of electronic energy bands in solids. The vacuum techniques employed allow operation of the spectrograph at pressures in the range 10^{-9}-10^{-10} mm Hg; these pressures are necessary in order to keep the specimen surface free from contamination. The apparatus is built almost entirely of 304 stainless steel and glass; it is completely bakeable. No ferromagnetic materials have been employed in the construction. It has been possible to make a number of stainless steel-to-glass seals that range from 3 inches to 0.25 inch in diameter.

The conventional diffraction grating would be risky to bake. A new dispersion system has therefore been designed which makes use of the Einstein relation between the velocity of a photo-ejected electron and the photon causing the ejection. A $(3\pi)/2$ electron spectrometer, which has been discussed previously (1), is used to analyze the photoelectrons. The photoelectric target for the soft X rays is a molecular beam. Magnesium is being used in preliminary studies.

Students have completed thesis work on an electron-injection system for an Allen type of multiplier for use with the spectrometer, and on the construction of an iron-free magnet based on previous calculations (1).

The electron spectrometer and its detection system have operated in initial tests according to calculations, and a resolution of 1 part in 1000 is expected. This may possibly be increased by electronic means, and it is hoped that such improvement will be limited only by stray magnetic fields.

A copper-beam oven has been developed for the purpose of laying down a copper surface in high vacuum. The band structure of this metal will be studied, and we hope that the M-levels may also be observed in the free atoms of the beam.

E. R. Pike, K. W. Billman

References

1. E. R. Pike, Focusing properties of a $3\pi/2$ electron spectrometer for studies of photoelectric emission excited by soft X rays, Quarterly Progress Report No. 53, Research Laboratory of Electronics, M.I.T., April 15, 1959, pp. 13-19.

B. CYCLOTRON RESONANCE IN N-TYPE GERMANIUM AT LIQUID-HELIUM TEMPERATURE

Measurement of cyclotron resonance in n-type germanium by exciting carriers with a dc electric field has shown two advantages over the methods of exciting carriers with light, or exciting carriers with the microwave electric field:

a. There is only one sign for the carrier, and it is possible to check the theory of cyclotron resonance developed by B. Lax (1) at lower ω/ν.

b. This method is less noisy than microwave excitation, and higher densities can be achieved than with the other two methods.

1. Method of Measurement and Results

The work in this quarter was devoted to improving both the accuracy and the interpretation of the measurements. The magnetic-field values and the effective mass parameters were measured in several samples of n-type germanium at magnetic fields greater than 683 gauss for $m_t = 0.08\ m_e$, where m_e is the mass of the free electron. The theoretical (1) and experimental values are listed below for two samples.

Sample 1

m^*/m_e

Theoretical	Experimental	
	B(111)	E(011)
0.205	1610	0.189
0.08	710	0.083

Sample 2

m^*/m_e

	B(211)	E(011)
0.358	>2700	>0.32
0.156	1220	0.143
0.08	663	0.078

Experimental studies were made to improve the accuracy of the ratio of microwave power absorbed at each separate resonance determined by the magnetic field. It is necessary to know n, the density of carriers, which is given by the relation $I_{dc} = ne\mu E_{dc}$; $n\mu$ occurs in a product, and μ was also measured separately from the

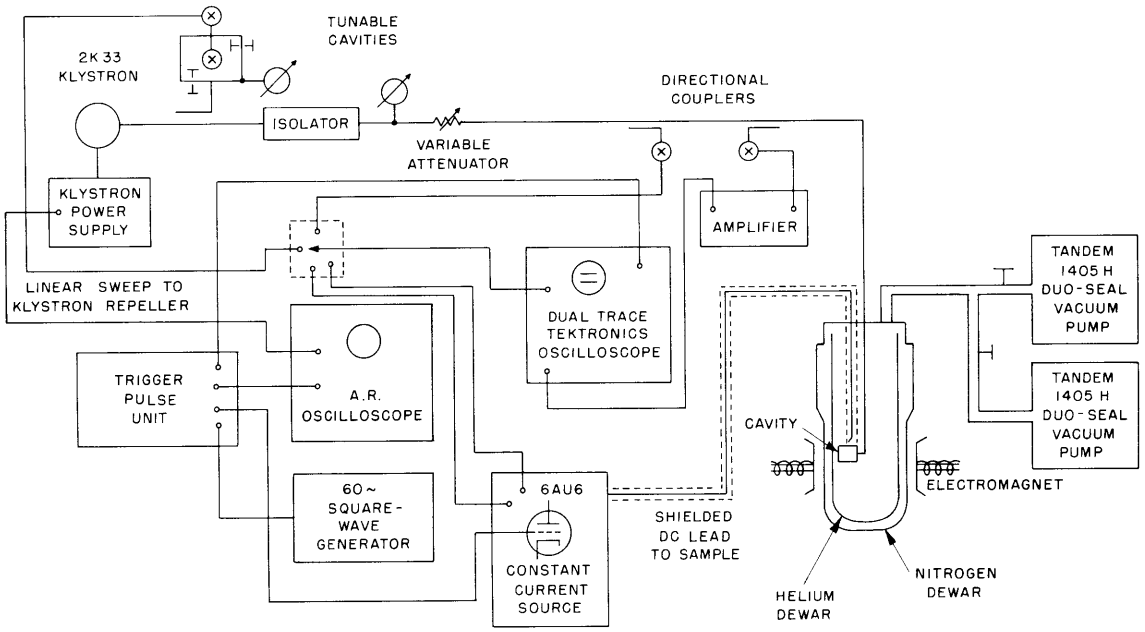

Fig. III-1. Schematic drawing of equipment used in cyclotron-resonance experiment.

magnetoresistance at T = 4.2°K. It was found that μ decreases monotonically when E_{dc} is perpendicular to B_{dc}, which is in agreement with magnetoresistance theory (2), and that μ decreases for B < 1800 gauss when E_{dc} and B_{dc} are parallel, and then remains constant as B increases. Figure III-1 shows the equipment used in the principal cyclotron-resonance experiment.

2. Theory of Anisotropic Scattering

In this investigation, the equation for the microwave conductivity of an electron in germanium for anisotropic scattering time has been solved, and it was found that with $\omega/\nu \sim 10$, the half-width of the cyclotron-resonance absorption is given by $\Delta = \nu_t - \frac{1}{2}\sin^2\theta\,\frac{m^{*2}}{m_t m_\ell}(\nu_t - \nu_\ell)$, where

$$\overleftrightarrow{\nu} = \begin{vmatrix} \nu_t & & \\ & \nu_t & \\ & & \nu_\ell \end{vmatrix}$$

and

$$\overleftrightarrow{m} = \begin{vmatrix} m_t & & \\ & m_t & \\ & & m_\ell \end{vmatrix}$$

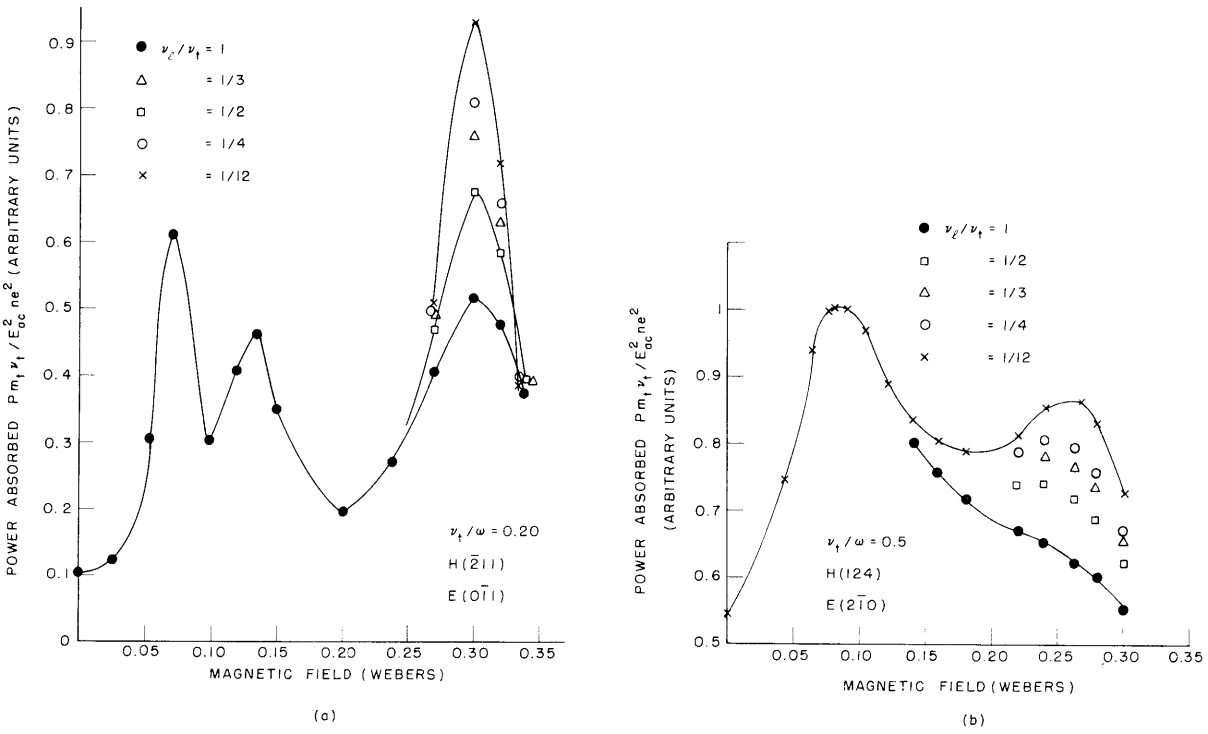

Fig. III-2. Microwave power absorption versus magnetic field for two magnetic-field orientations.

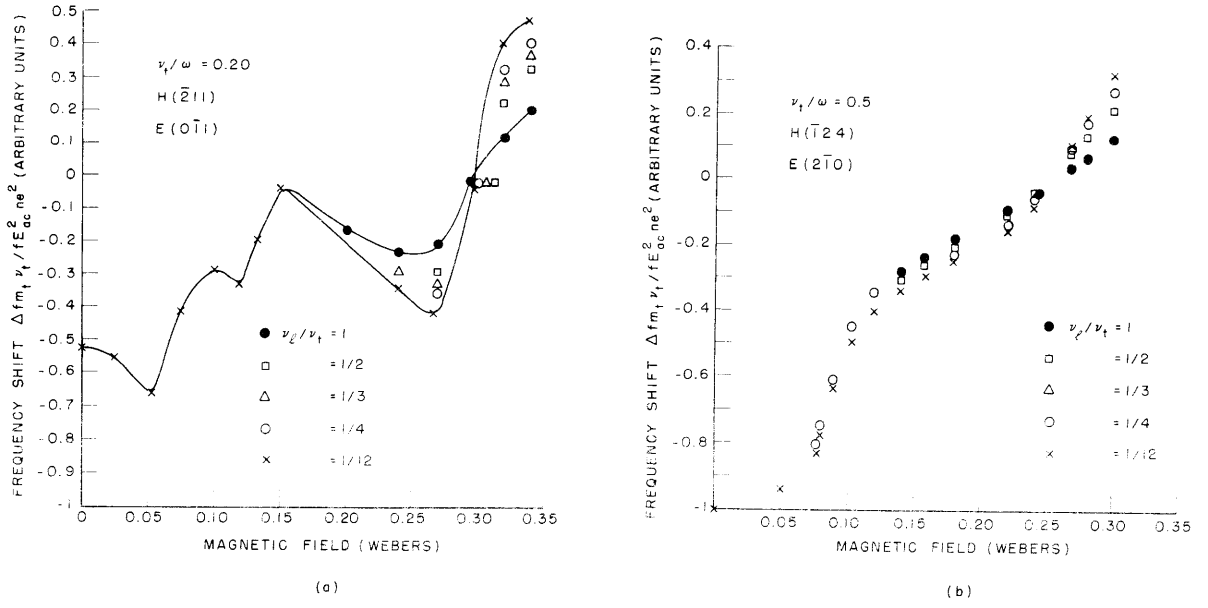

Fig. III-3. Microwave frequency shift versus magnetic field for the two magnetic-field orientations of Fig. III-2.

Here, θ is the angle that the B-field makes with the 111 direction.

Formulas for the frequency shift and power absorption were computed numerically for $\omega/\nu = 2.5, 3, 4, 5$, and for $\nu_\ell/\nu_t = \frac{1}{12}, \frac{1}{4}, \frac{1}{3}, \frac{1}{2}$, with $\omega = 23.4 \times 10^9 \times 2\pi$. Plots of microwave power absorption versus magnetic field (Figs. III-2 and III-3) have been made with the aid of the following formula calculated for power absorption and frequency shift of the resonant cavity containing germanium:

$$\frac{P}{ne^2E_{ac}^2/m_t\nu_t} = \frac{\dfrac{\sin^2\phi}{\left(1+\frac{\omega^2}{\nu_t^2}\right)} + \dfrac{\cos^2\phi\,\frac{\nu_\ell}{\nu_t}}{\frac{m_\ell}{m_t}\left[\left(\frac{\nu_\ell}{\nu_t}\right)^2+\frac{\omega^2}{\nu_t^2}\right]} + \dfrac{\omega_{bt}^2}{\nu_t^2\left(1+\frac{\omega^2}{\nu_t^2}\right)}\left[\dfrac{\sin^2\phi\sin^2\theta\,\frac{\nu_\ell}{\nu_t}}{\frac{m_\ell}{m_t}\left[\left(\frac{\nu_\ell}{\nu_t}\right)^2+\frac{\omega^2}{\nu_t^2}\right]} + \dfrac{\sin^2\phi\cos^2\theta}{\left[1+\frac{\omega^2}{\nu_t^2}\right]} + \dfrac{\cos^2\phi\sin^2\theta}{\left(\frac{m_\ell}{m_t}\right)\left[\left(\frac{\nu_\ell}{\nu_t}\right)^2+\frac{\omega^2}{\nu_t^2}\right]} + \dfrac{\cos^2\phi\cos^2\theta\left[\frac{\nu_\ell}{\nu_t}+\frac{2\omega^2}{\nu_t^2}-\frac{\omega^2}{\nu_t^2}\frac{\nu_\ell}{\nu_t}\right]}{\left(\frac{m_\ell}{m_t}\right)\left[\left(\frac{\nu_\ell}{\nu_t}\right)^2+\frac{\omega^2}{\nu_t^2}\right]\left[1+\frac{\omega^2}{\nu_t^2}\right]}\right]}{1+\dfrac{\omega_{bt}^2}{\nu_t^2\left(1+\frac{\omega^2}{\nu_t^2}\right)}\left[\dfrac{2\sin^2\theta\left[\frac{\nu_\ell}{\nu_t}-\frac{\omega^2}{\nu_t^2}\right]}{\frac{m_\ell}{m_t}\left[\left(\frac{\nu_\ell}{\nu_t}\right)^2+\frac{\omega^2}{\nu_t^2}\right]} + \dfrac{2\cos^2\theta\left[1-\frac{\omega^2}{\nu_t^2}\right]}{\left(1+\frac{\omega^2}{\nu_t^2}\right)} + \dfrac{\omega_{bt}^2}{\nu_t^2}\left\{\dfrac{\sin^4\theta}{\left(\frac{m_\ell}{m_t}\right)^2\left[\left(\frac{\nu_\ell}{\nu_t}\right)^2+\frac{\omega^2}{\nu_t^2}\right]} + \dfrac{2\sin^2\theta\cos^2\theta\left[\frac{\nu_\ell}{\nu_t}+\frac{\omega^2}{\nu_t^2}\right]}{\frac{m_\ell}{m_t}\left(1+\frac{\omega^2}{\nu_t^2}\right)\left[\left(\frac{\nu_\ell}{\nu_t}\right)^2+\frac{\omega^2}{\nu_t^2}\right]} + \dfrac{\cos^4\theta}{\left(1+\frac{\omega^2}{\nu_t^2}\right)}\right\}\right]} \tag{1}$$

$$\frac{\Delta f}{nfe^2E_{ac}^2/m_t\nu_t\epsilon_o\omega} = -1\left(\frac{\omega}{\nu_t}\right)\frac{\dfrac{\sin^2\phi}{\left(1+\frac{\omega^2}{\nu_t^2}\right)} + \dfrac{\cos^2\phi}{\frac{m_\ell}{m_t}\left[\left(\frac{\nu_\ell}{\nu_t}\right)^2+\frac{\omega^2}{\nu_t^2}\right]} - \dfrac{\omega_{bt}^2}{\nu_t^2\left(1+\frac{\omega^2}{\nu_t^2}\right)}\left\{\dfrac{\sin^2\phi\sin^2\theta}{\frac{m_\ell}{m_t}\left[\left(\frac{\nu_\ell}{\nu_t}\right)^2+\frac{\omega^2}{\nu_t^2}\right]} + \dfrac{\sin^2\phi\cos^2\theta}{\left(1+\frac{\omega^2}{\nu_t^2}\right)} + \dfrac{\cos^2\phi\sin^2\theta}{\left(\frac{m_\ell}{m_t}\right)\left[\left(\frac{\nu_\ell}{\nu_t}\right)^2+\frac{\omega^2}{\nu_t^2}\right]} + \dfrac{\cos^2\phi\cos^2\theta\left[\frac{\omega^2}{\nu_t^2}+\frac{2\nu_\ell}{\nu_t}-1\right]}{\frac{m_\ell}{m_t}\left[\left(\frac{\nu_\ell}{\nu_t}\right)^2+\frac{\omega^2}{\nu_t^2}\right]\left[1+\frac{\omega^2}{\nu_t^2}\right]}\right\}\right]}{1+\dfrac{\omega_{bt}^2}{\nu_t^2\left(1+\frac{\omega^2}{\nu_t^2}\right)}\left[\dfrac{2\sin^2\theta\left[\frac{\nu_\ell}{\nu_t}-\frac{\omega^2}{\nu_t^2}\right]}{\frac{m_\ell}{m_t}\left[\left(\frac{\nu_\ell}{\nu_t}\right)^2+\frac{\omega^2}{\nu_t^2}\right]} + \dfrac{2\cos^2\theta\left[1-\frac{\omega^2}{\nu_t^2}\right]}{\left(1+\frac{\omega^2}{\nu_t^2}\right)} + \dfrac{\omega_{bt}^2}{\nu_t^2}\left\{\dfrac{\sin^4\theta}{\left(\frac{m_\ell}{m_t}\right)^2\left[\left(\frac{\nu_\ell}{\nu_t}\right)^2+\frac{\omega^2}{\nu_t^2}\right]} + \dfrac{2\sin^2\theta\cos^2\theta\left[\frac{\nu_\ell}{\nu_t}+\frac{\omega^2}{\nu_t^2}\right]}{\frac{m_\ell}{m_t}\left(1+\frac{\omega^2}{\nu_t^2}\right)\left[\left(\frac{\nu_\ell}{\nu_t}\right)^2+\frac{\omega^2}{\nu_t^2}\right]} + \dfrac{\cos^4\theta}{\left(1+\frac{\omega^2}{\nu_t^2}\right)}\right\}\right]} \tag{1}$$

The plots showed, first, that the power P can be represented by a simpler formula:

$$P = E_{ac}^2\frac{n_e^2}{m_t\nu_t}\sum\alpha_i\left[\frac{1}{1+(\omega-\omega_{bi})^2/\nu_i^2} + \frac{1}{1+(\omega-\omega_{bi})^2/\nu_i^2}\right] \tag{2}$$

where $\alpha_i = \sin^2\phi_i + \cos^2\dfrac{\phi_i}{m_\ell/m_t}$, and $\nu_i = \nu_t - \frac{1}{2}\sin^2\phi_i\dfrac{m^{*2}}{m_t m_\ell}(\nu_t-\nu_\ell)$.

The plots also showed that at B = 3000 gauss, the difference in microwave power absorption with isotropic scattering and anisotropic scattering can be as high as 80 per cent. Thus a reasonably accurate comparison of the power-absorption maxima,

$$\frac{P_{B=700}}{P_{B=3000}} = A$$

gives a good indication of whether or not the anisotropic scattering is an effective mechanism.

T. Higier

References

1. B. Lax, R. N. Dexter, A. F. Kip, and G. Dresselhaus, Effective masses of electrons in silicon, Phys. Rev. 96, 222 (1954).

2. L. Gold, Anisotropy of the hot electron problem in semi-conductors with spheroidal energy surfaces, Phys. Rev. 104, 1580 (1956).